

Assessment of long-term extreme response of a floating support structure using the environmental contour method

K. Raed, A.P. Teixeira & C. Guedes Soares

Centre for Marine Technology and Ocean Engineering (CENTEC), Instituto Superior Técnico, Universidade de Lisboa, Lisbon, Portugal

ABSTRACT: This paper analyses the extreme response of a semi-submersible floating support structure for a wind turbine installed in the northern North Sea. The environmental contour method is used to directly estimate the extreme sea states that are used thereafter to calculate the long-term extreme response of the semi-submersible. This study focuses on the 1D and 2D environmental contours model based on the inverse first-order reliability method (IFORM). The significant wave height and peak period are the two environmental random variables used to estimate the contour. The response amplitude operator of the heave, surge, and pitch in head waves are estimated using the 3D panel method. A full long-term analysis is performed and compared with that estimated by adopting the 1D and 2D model. The results show a remarkable deviation between the full long-term analysis and the long-term obtained by the environmental contour method except in the heave response.

1 INTRODUCTION

Estimating the long-term extreme responses is of crucial importance in the reliability-based design of any floating offshore wind turbine. Among others, two uncertainties are associated with such a structural reliability problem: (1) the environmental load, and the (2) extreme response. In an attempt to decouple these uncertainties, Winterstein et al. (1993) presented a method to construct environmental contours based on the inverse first-order reliability method (FORM). Nowadays, the FORM is widely used to solve and analyses reliability problems for ships and offshore structures, e.g. Teixeira & Guedes Soares (2005), Teixeira & Guedes Soares (2009) and Guedes Soares et al. (2010).

The general idea of constructing environmental contour is based on identifying the extreme sea states corresponding to a certain probability of failure (P_f) and using these values to calculate the long-term extreme response. Winterstein & Engebretsen (1998) applied this concept and described procedures to estimate the extreme design loads and response for both spar buoy and a tension leg platform (TLP). However, it has been noted that neglecting the response variability in these procedures underestimates the extreme response, e.g. in case of the TLP, the median of the 100-year return period response was under estimated by 1.3 to 1.4 times compared to the actual response, whereas these values were much more in the spar buoy case. Since this method was accurate enough, many researchers adopted it in wind turbine applications.

Karmakar et al. (2016) used the aforementioned environmental contour approach to investigate the long-term extreme bending moments acting on the turbine's blade root and on the tower base for a spar and a semi-submersible type of floaters. They took into consideration the wind speed, the significant wave height and the peak period. Agarwal & Manuel (2009) determined the long-term extreme load acting on the offshore wind turbine foundation using an efficient inverse reliability approach. Furthermore, Karimirad & Moan (2011) focused on the extreme coupled wind and wave induced motion for a floating offshore wind turbine of a spar type.

However, the results of the conventional environmental contour method for some responses of wind turbines have been also found to be largely under-predicted as shown by Saranyasoontorn & Manuel (2004), Agarwal & Manuel (2009) and Li et al. (2016). Li et al. (2017) overcame this problem by presenting a modified environmental contour method (MECM), which is also based on the FORM considering the active survival strategy to be better suited for offshore wind turbines. The environmental contour can be 1D, 2D or 3D depending on the number of environmental random variables taken into consideration.

In this study only the 1D and 2D contour are considered. In order to construct the contours of the environmental parameters, it is necessary to identify the joint distribution of the environmental parameters. Many studies have been done on the joint distribution of significant wave height (H_s) and wave period (T_p) in the northern North Sea, which results in a marginal Weibull distribution for

H_s and a log-normal conditional distribution for T_p , e.g. Haver (1985), Ferreira & Guedes Soares (2002), DNV (2010), Vanem & Bitner-Gregersen (2015) and Lucas & Guedes Soares (2015).

Alternatively, a full long-term analysis could be done instead of the environmental contour method. The full long-term analysis combines the response distributions of all short-term environmental conditions according to their probability of occurrence. Guedes Soares (1993) and Guedes Soares & Schellin (1996) proposed a methodology for the long-term formulation of non-linear wave induced vertical bending moment. Furthermore, Chakrabarti (2005) and Nejad et al. (2013) described three different approaches to estimate characteristic long-term extreme values based on all peak values, all short term extreme values and the up-crossing rate.

The disadvantage of this method is the large number of simulations required, which is considered by Videiro & Moan (1999) not efficient. Furthermore, Raed et al. (2016) adopted the full long-term analysis to estimate the long-term Morison's wave load acting on the OC4 floating structure. In order to reach the final stage for these calculations, it was necessary to estimate the Response Amplitude Operators (RAO) of the floating structure. To do that, the linear frequency-domain analysis was adopted in this study and a detailed explanation for this type of analysis is described by Newman (1977), Falinsen (1990).

This paper presents the long-term extreme response acting on the OC4 wind turbine floating support structure (semi-submersible) located in the northern North Sea. The one-dimensional and the two-dimensional environmental contour models based on the inverse FORM are adopted to estimate the long-term extreme response for the semi-submersible. The significant wave height and the peak period are the environmental variables considered in this study. The Weibull distribution is adopted for H_s and a log-normal distribution for T_p as done by Haver (1985). ANSYS AQWA is used to predict the heave, surge, and pitch RAOs. Thereafter, the responses are estimated by multiplying the JONSWAP spectrum for each sea state (H_s, T_p) by the square of the RAO. The long-term extreme response resulting from the 1D and 2D environmental model are compared with the fully long-term analysis based the scatter diagram in the northern North Sea, (Moan et al. 2005).

2 RELIABILITY BASED ANALYSIS

The limit state function for any reliability problem can be defined as follows:

$$g(x) = y_{capacity} - Y(x) \quad (1)$$

where $g(x)$ is the limit state function; $y_{capacity}$ is the strength; and the $Y(x)$ is the load acting on the structure. The reliability (R) is related to the probability of failure (P_f) and the relation is given by:

$$R = 1 - P_f = P[g(x) > 0] = \int_{g(x) > 0} f_x(x) dx \quad (2)$$

Since this integration is often difficult to solve due to the complicated joint distribution of the random variables. The first-order reliability method (FORM) and second-order reliability method (SORM), (see Melchers 1999 for more details). The relation between the reliability index (β) and the probability of failure (P_f) is given by:

$$\beta = \Phi^{-1}(1 - P_f) \quad (3)$$

where Φ is the standard Gaussian probability distribution.

2.1 Environmental contour

The environmental contour method is an effective, risk-based, time saving approach. The widely used environmental contour method is based on the Rosenblatt transformation. This is done by transforming the vector of environmental variables, \mathbf{X} , into a vector \mathbf{U} of independent normally distributed variable, (Vanem 2017). Figure 1 illustrates the concept of transformation. This method is based on the inverse FORM since the P_f is assumed despite of computed.

The probability of failure (P_f) is given by:

$$P_f = \frac{T_{ss}}{365 \cdot 24 \cdot T_r} \quad (4)$$

where T_{ss} is the sea state duration in hours; T_r is the return period in years; and the (360×24) factor is to convert the number of years to hours. If the joint density function of all variables is known the transformation of original design variables (dependent and non-normal) to independent standard normal variables can be performed using the Rosenblatt transformation as will be described below.

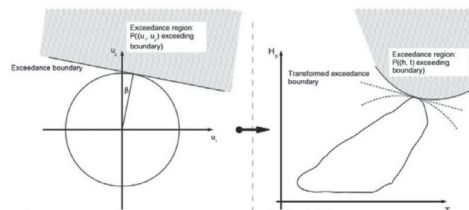


Figure 1. Illustration of the transformation from the normal space to the physical space, Huseby et al. (2013).

2.1.1 One-dimensional (1D) model

In case of the 1D model the reliability index (β) is assumed to be equal to random variable (u_i) in the normal space, as shown in

Figure 2 and the other environmental random variables are assumed to be zero.

According to the 1-D model, the probability of exceedance is related to the standard normal space by:

$$u_1 = \beta; u_2 = 0; u_3 = 0 \tag{5}$$

where β is the reliability index related to the failure probability (P_f) by eq.(3). Thereafter, using the Rosenblatt transformation scheme, the physical plan's points are obtained by:

$$\begin{aligned} \Phi(u_1) &= F_X(X_1) \\ \Phi(0) &= F_{X_2|X_1}(X_2|X_1) \end{aligned} \tag{6}$$

2.1.2 Two-dimensional model

In the two-dimensional environmental contour model, the random variables in the normal space are assumed to be in a circle with radius equal to β , as shown in Figure 3.

where u_i and u_2 are given by:

$$u_1 = \beta \cos \theta; u_2 = \beta \sin \theta; u_3 = 0 \tag{7}$$

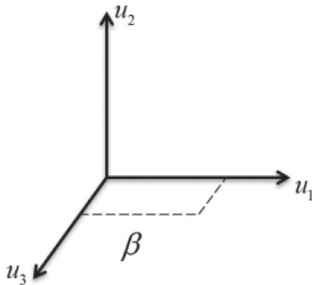


Figure 2. One dimensional model illustration; (Karmakar et al. 2016).

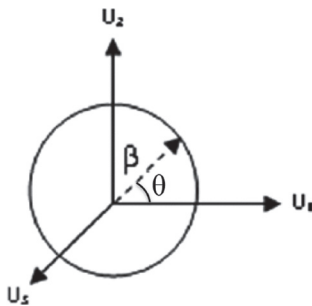


Figure 3. Geometric representation of the 2D model representation in the U-space, (Karmakar et al. 2016).

where θ is the angle between β and u_i , and vary between $0^\circ < \theta < 360^\circ$.

Similarly, by applying the Rosenblatt transformation, the physical plan points are obtained by:

$$\begin{aligned} \Phi(u_1) &= F_X(X_1) \\ \Phi(u_2|u_1) &= F_{X_2|X_1}(X_2|X_1) \end{aligned} \tag{8}$$

Hence, for a given marginal distribution for X_i and conditional distribution for X_2 , the Rosenblatt transformation results in:

$$\begin{aligned} X_1 &= F_X^{-1}(\Phi(u_1)); \\ X_2|X_1 &= F_{X_2|X_1}^{-1}(\Phi(u_2|u_1)) \end{aligned} \tag{9}$$

where the joint distribution of the two environmental parameters (X_1, X_2) are given in the next section.

2.2 Joint probability distribution of H_s and T_p

The marginal distribution of the significant wave height $F_{H_s}(h)$ is given by the Weibull distribution as follows: (Winterstein et al. 1993)

$$F_{H_s}(h) = 1 - \exp\left(-\left(\frac{h}{2.822}\right)^{1.547}\right) \tag{10}$$

whereas the conditional distribution of the peak period $F_{T_p|H_s}(T_p|H_s)$ is given by a log-normal distribution, which has mean and variance as follows: (Winterstein et al. 1993)

$$\mu = E(T_p|H_s) = 1.59 + 0.42 \ln(H_s + 2) \tag{11}$$

$$Var = 0.005 + 0.085 \exp(-0.13 H_s^{1.34}) \tag{12}$$

3 RESPONSE IN IRREGULAR WAVES

The general equation of motion for the system is:

$$(\mathbf{M} + \mathbf{A})\ddot{\zeta} + \mathbf{B}\dot{\zeta} + \mathbf{C}\zeta = \mathbf{F}(t) \tag{13}$$

Table 1. Fitted parameters for the 2 parameters Weibull distribution for H_s and conditional log-normal distribution for T_p according to Eqs. (10), (11) and (12); Northern North Sea.

Weibull (H_s)	Shape	Scale		
	1.547	2.822		
Lognormal (T_p)	μ	a1	a2	a3
	σ^2	b1	b2	b3
	0.005	0.085	-0.13	1.34

where \mathbf{M} is the mass of the structure; \mathbf{A} is the added mass matrix; \mathbf{B} and \mathbf{C} are the damping coefficient and the restoring coefficient respectively; \mathbf{F} is the hydrodynamic excitation; ζ is the semi-submersible displacement from its mean position. The response of a linear motion is obtained by multiplying the wave energy spectrum $S_w(\omega)$ by the square of RAO for the appropriate motion as follows:

$$S_R(\omega) = S_w(\omega)RAO_j^2(\omega) \quad (14)$$

$$RAO(\omega) = \left(\frac{x_j}{\zeta_{wave}} \right) \quad (15)$$

where x_j is the motion displacement and ζ_{wave} is the wave amplitude in [m]

3.1 JONSWAP Spectrum

The Joint North Sea Wave Project (JONSWAP) spectrum is used in this study to estimate the energy of the sea state in the northern North Sea. The JONSWAP spectrum is given by: (Journée & Massie 2001)

$$S(\omega) = \frac{320H_s^2}{T_p^4} \omega^{-5} \exp\left(\frac{-1950}{T_p^4} \omega^{-4}\right) \gamma^A \quad (16)$$

where

$$A = \exp\left\{-\left(\frac{\frac{\omega}{\omega_p} - 1}{\frac{\omega_p}{\sigma\sqrt{2}}}\right)^2\right\} \quad (17)$$

where ω is the wave frequency in rad/sec; γ is the peakedness factor and is equal to 3.3; ω_p is the peak period in rad/sec and is given by:

$$\begin{aligned} \omega_p &= \frac{2\pi}{T_p} \\ \sigma &= 0.07 \quad \text{if } \omega < \omega_p \\ \sigma &= 0.09 \quad \text{if } \omega > \omega_p \end{aligned}$$

4 FULL LONG-TERM ANALYSIS

The idea behind the long-term extreme load analysis is to obtain an estimation of the extreme load with a given probability of exceedance by accounting the load from various short-term wave conditions, as presented by Guedes Soares (1998). The probability of exceeding a given level x of wave amplitude is given by the Rayleigh distribution as:

$$Q_s(X|R) = \exp\left(\frac{-x^2}{2R}\right), \quad (18)$$

where R is the variance of the process. The Gaussian process assumes that in the frequency domain the process is completely described by its power spectrum. So, the area under the spectrum is directly related to the variance. The variance (R) for each combination of parameters is given by:

$$R = m_0 = \int_0^\infty S_R(\omega, H_s, T_p, D, h, Z, H) \quad (19)$$

where S_R is the response spectrum which is given by eq. (14), ω is the wave frequency, H_s is the significant wave height, T_p is the peak period, D is the member diameter, h is the water depth, Z is the draft and H is the wave height. The basic formulation applicable to calculate the long-term distribution of wave amplitude is given by:

$$Q_L = \int_0^\infty Q_s(x|r) \cdot f_R(r) dr \quad (20)$$

where Q_s is the short-term distribution given by eq.(18) and f_R is the probability density function of the sea state variance and is obtained from the scatter diagram. The number of years corresponds to the full long-term distribution is given also by eq. (4).

5 RESULTS AND DISCUSSION

The model of the semi-submersible used in this study is shown in Figure 4, which consists of three side columns and one main column that support the wind turbine. Table 2 shows the main characteristics of the floating structure as prescribed by Robertson et al. (2014).

The analysis was made using ANSYS AQWA to estimate the heave, surge and pitch RAOs in head waves. The environmental variables under consideration are the significant wave height (H_s) and the peak

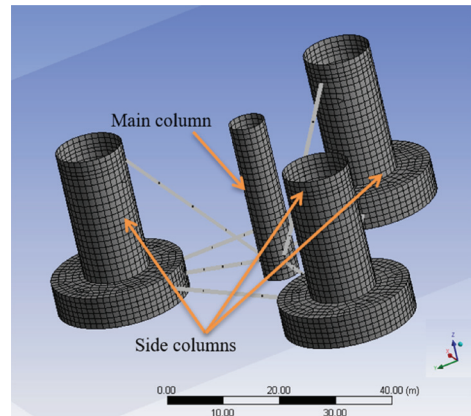


Figure 4. Semi-submersible geometry.

Table 2. Main characteristics of the OC4 semi-submersible.

Main Column diameter	6.5 m
Offset column diameter	12 m
Bottom column diameter	24 m
Bracing diameter	1.6 m
Draft	20 m
Mass including ballast	1.3473E+7 kg
Center of mass below SWL	13.46 m
Roll moment of inertia I_{xx} about COG	6.827E+9 kg.m ²
Pitch moment of inertia (I_{yy}) about COG	6.827E+9 kg.m ²
Yaw moment of inertia (I_{zz}) about COG	1.226E+10 kg.m ²

period (T_p). Regarding the 1D model, H_s is considered as random and T_p is estimated directly from the log-normal distribution by substituting the H_s value corresponding to each P_f . The probability of failure is calculated using eq.(4) for each return period (T_r) and for T_{ss} equal to 3 hours. Thereafter, the reliability index (β) estimated for 10 years return period is 3.98, 4.19 for 25-years return period, whereas for 50 and 100 years are 4.35 and 4.5, respectively, as shown in Table 3. Winterstein et al. (1993) presented the Weibull distribution parameters and the lognormal distribution parameters for H_s and T_p , respectively as shown in the aforementioned Table 1.

Adopting the 1D environmental contour model results in increasing H_s as the return period increases as shown in the left-hand plot of Figure 5. Comparing the results obtained for the 25, 50 and 100 years, it is observed that increasing the return period by 50% results in increasing the values of H_s by 3.7% and the T_p by 1.2% on average, as shown in the right-hand plot of Figure 5. It can be noted that, the behaviour of the H_s and T_p is nearly linear since T_p increases with increasing H_s .

The 2D environmental contour model differs from the 1D model in the number of the variable's points (H_s, T_p) constructing the contour. The 1D model results in only one point for each return period, whereas, the 2D environmental contour results in a large number of points depend on the tangent lines around the circle of radius β in the normal space (Figure 1). Figure 6 shows the 2D environmental contour using the inverse first-order reliability method (IFORM) for 10, 25, 50 and 100 years return period based on 60 tangent lines. The number of tangent lines selected gives reasonable and visually smooth contours, as shown in Figure 6.

Table 4 shows the values of (H_s, T_p) along the contours for 10, 25, 50 and 100-years using the 2D model approach. Only the values up to 102 degrees are presented since higher angles result in lower values for H_s and T_p . These contour values will be used in the response analysis of heave, surge and pitch motions

Table 3. Values of the 1D environmental contour.

Return period [yrs.] (Pf)	(β)	Hs [m]	Tp [s]
10	1.141E-05	3.98	12.73
25	4.566E-06	4.19	13.45
50	2.283E-06	4.35	13.98
100	1.142E-06	4.50	14.50

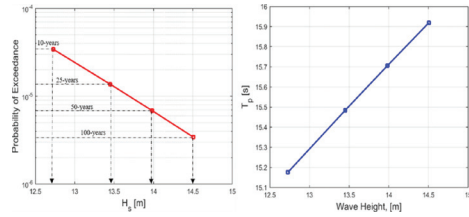


Figure 5. 1D environmental contour.

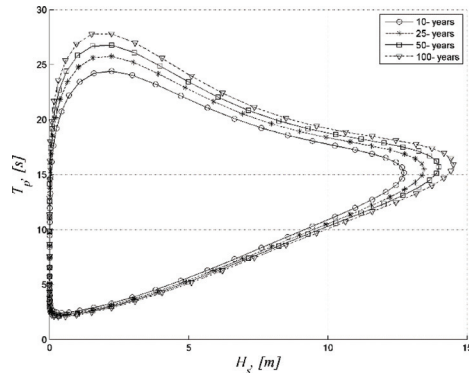


Figure 6. 2D contour using inverse FORM.

for the semi-submersible under consideration. The 100-years extreme condition estimated by Winterstein et al. (1993) was $H_s = 14.5$ m and $T_p = 15.9$ s, and it can be observed that this value agrees well with the values shown in Table 4. As expected, the maximum values of H_s and their corresponding T_p 's values obtained by the 2D model at 0° are identical to those obtained by the 1D model. Despite that, the extreme response will not be obtained at the maximum H_s values as will be shown later.

As shown in Table 4, increasing the return period by 50% (e.g. from 25 years to 50 years) results in increasing the H_s by 3.13% on average between the intervals $[0^\circ, 90^\circ]$ and $[270^\circ, 360^\circ]$, while decreasing the H_s by 20.41% on average in the interval $[90^\circ, 270^\circ]$. Regarding the conditional T_p , increasing the return period in general tends to increase its values except in the interval $[180^\circ, 300^\circ]$. Strictly, increasing the return period from 25 to 50 years lead to increase the T_p by 1.46% on average and decrease it by 2.9% on average in the interval $[180^\circ, 300^\circ]$.

Table 4. Points selected along the 2D environmental contour.

θ°	(H_s, T_p)			
	10-years	25-years	50-years	100-years
0	(12.73, 15.18)	(13.45, 15.48)	(13.98, 15.71)	(14.50, 15.92)
6	(12.66, 15.67)	(13.37, 16.00)	(13.90, 16.23)	(14.42, 16.46)
12	(12.44, 16.12)	(13.14, 16.46)	(13.65, 16.71)	(14.16, 16.9)
18	(12.08, 16.53)	(12.75, 16.88)	(13.25, 17.14)	(13.74, 17.39)
24	(11.59, 16.90)	(12.23, 17.26)	(12.70, 17.52)	(13.16, 17.78)
30	(10.97, 17.27)	(11.57, 17.62)	(12.01, 17.88)	(12.44, 18.14)
36	(10.25, 17.64)	(10.8, 17.99)	(11.20, 18.24)	(11.59, 18.49)
42	(9.44, 18.07)	(9.93, 18.41)	(10.28, 18.66)	(10.64, 18.89)
48	(8.55, 18.60)	(8.98, 18.94)	(9.29, 19.18)	(9.59, 19.42)
54	(7.61, 19.26)	(7.97, 19.63)	(8.23, 19.89)	(8.49, 20.14)
60	(6.64, 20.10)	(6.93, 20.54)	(7.15, 20.84)	(7.36, 21.13)
66	(5.67, 21.09)	(5.89, 21.65)	(6.06, 22.05)	(6.21, 22.42)
72	(4.72, 22.18)	(4.87, 22.92)	(4.99, 23.45)	(5.10, 23.96)
78	(3.81, 23.23)	(3.90, 24.19)	(3.97, 24.90)	(4.04, 25.58)
84	(2.97, 24.05)	(3.01, 25.23)	(3.04, 26.11)	(3.08, 26.99)
90	(2.23, 24.43)	(2.23, 25.77)	(2.23, 26.79)	(2.23, 27.82)
96	(1.59, 24.23)	(1.56, 25.63)	(1.54, 26.70)	(1.52, 27.79)
102	(1.09, 23.44)	(1.04, 24.80)	(1.00, 25.84)	(0.97, 26.90)

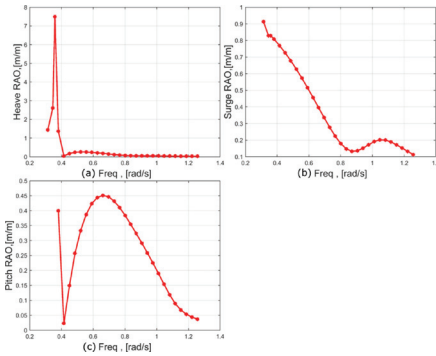


Figure 7. (a) Heave RAO, (b) Surge RAO and (c) Pitch RAO.

The linear body response in the frequency-domain was estimated by calculating the motions Response Amplitude Operator (RAO) of the semi-submersible using ANSYS AQWA. The numerical model was analysed in a frequency range between 0.34 rad/s and 1.25 rad/s. Figure 7 shows the RAOs at zero-degree wave heading of the motions under consideration; plot (a), (b) and (c) present the heave, surge and pitch motion, respectively.

Regarding the heave RAO, as expected, at low frequencies the semi-submersible has an amplitude equal to the exciting waves. Moreover, the heave excitation is maximum at the heave natural frequency (0.36 rad/s) and reaches 7.2 m/m which compare well with some of the results published in Robertson et al. (2014). The surge and pitch RAOs are shown in Figure 7(b) and (c), respectively. It can be noted the pitch-surge coupling through the peak

at the pitch natural frequency (0.32 rad/s). Furthermore, it is expected that the peak in the pitch-surge coupling in the no-wind case, which is the case under consideration, is higher than if we consider the wind turbine installed and in an operation condition.

Table 5 shows the response values of the three modes of motion under consideration (heave, surge and pitch) resulting from adopting the 1D environmental contour model. As expected, the 100-years return period, which is equivalent to $\beta = 4.5$ always gives the highest response corresponds to the highest sea state. However, the 1D model results in only one extreme sea state that causes the extreme response for all motions under consideration at the same time, which is not realistic. It can be observed that increasing the return period by 50% results in increasing the heave, surge and pitch responses by 11%, 4% and 10.7% on average, respectively.

The 2D environmental contour results are presented in Table 6 and Table 7. It can be observed that the maximum response for each motion corresponds to a different sea state.

Table 5. Long-term extreme response results from the 1D model.

Return period [yrs.]	1D model				
	H_s [m]	T_p [s]	Heave [m]	Surge [m]	Pitch [°]
10	12.73	15.18	8.78	1.68	0.66
25	13.45	15.48	10.26	1.75	0.79
50	13.98	15.71	11.54	1.77	0.89
100	14.50	15.92	12.95	1.90	0.99

Table 6. Long-term extreme response results from the 2D model (heave and pitch motions).

Return period [yrs.]	Heave motion			Pitch motion		
	H_s [m]	T_p [s]	amp [m]	H_s [m]	T_p [s]	amp [°]
10	10.97	17.27	14.88	12.08	16.53	0.91
25	12.23	17.26	16.56	13.14	16.46	0.99
50	13.25	17.14	17.62	13.65	16.71	1.03
100	13.74	17.40	18.87	14.42	16.46	1.09

Table 7. Long-term extreme response results from the 2D model (surge motion).

Return period [yrs.]	Surge motion		
	H_s [m]	T_p [s]	amp [m]
10	12.08	16.53	1.75
25	13.14	16.46	1.90
50	13.65	16.71	1.97
100	13.74	17.34	2.09

In case of 50-years return period, the heave maximum response is equal to 14.9 m and is obtained in a sea state (11 m, 17 s), while the pitch maximum response is equal to 0.90 and occurring at a sea state (12.1 m, 16.5 s). Increasing the return period by 50% results in higher the extreme amplitude of heave, pitch and surge by 6.3%, 4.7% and 4.6% on average, respectively.

Figure 8, Figure 9 and Figure 10 illustrate a comparison between the extreme response for the semi-submersible obtained by the 1D model, the 2D model and the full long-term analysis in the northern North Sea for the heave, surge and pitch responses, respectively. Regarding the heave response shown in Figure 8, the full long-term analysis agrees well with the 2D model results until approximately 30-years return period. Thereafter, the results diverge until the end.

The full-long term analysis overestimates the heave response's value by around 10%, after 30-yr return period, compared to the 2D model, whereas the 1D model strongly under predicts the results. In Figure 9 and Figure 10, the results show that the

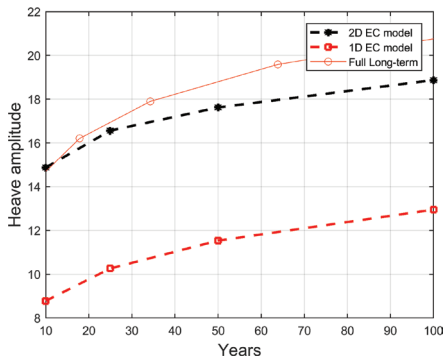


Figure 8. Comparison between the results obtained by both the 1D and 2D model with the full long-term analysis for heave response.

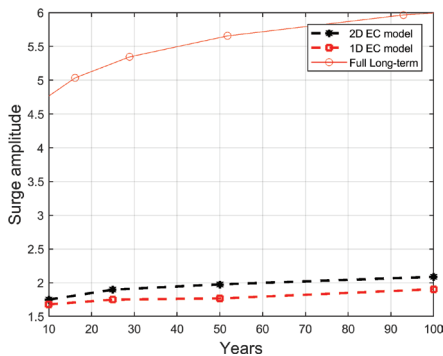


Figure 9. Comparison between the results obtained by both the 1D and 2D model with the full long-term analysis for surge response.

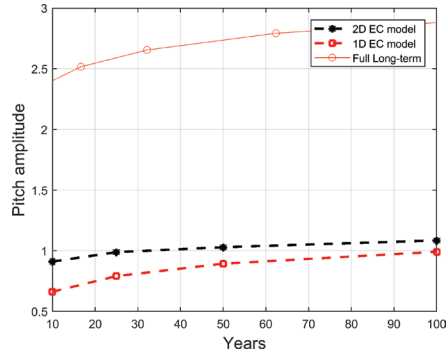


Figure 10. Comparison between the results obtained by both the 1D and 2D model with the full long-term analysis for pitch response.

full long-term analyses result in 65% and 72% higher response for the surge and pitch, respectively compared to the 2D model. On the other hand, the results obtained by adopting the 1D and 2D model agree well with each other's as shown in Figure 9 and Figure 10.

6 CONCLUSIONS

In the present study, the 1D and 2D environmental contour models based on the IFORM are used to estimate the extreme sea states in the northern North Sea. The long-term extreme responses, for the heave, surge and pitch responses of a semi-submersible are estimated by multiplying the JONSWAP spectrum by the RAOs obtained from ANSYS AQWA. Moreover, the long-term obtained by adopting both the 1D and 2D models are compared with those estimated by the full long-term approach.

The 1D model results in a nearly linear significant wave height behaviour and accordingly peak period behaviour. This behaviour is no longer linear with the 2D model. 60 tangent lines are used to construct the 2D environmental contours, which results in a visually smooth contour.

The 1D model compares well with the 2D model in the linear behaviour. Adopting the 1D model results in increasing Hs by 3.7% and Tp by 1.2%, whereas adopting the 2D results in increasing Hs by 3.13% and Tp by 1.46% in the linear domain.

The 2D model produces more realistic results than the 1D model. The later results in a maximum heave, surge and pitch response at only one sea state. However, the 2D model provides the sea states that causes the maximum of each response individually.

The results of the environmental contour method and the full long-term analysis are also compared. A remarkable deviation is observed, which agree well with Saranyasoontorn & Manuel (2004), except for the heave long-term response. This is expected due to the peak periods resulting

from the 2D model, that are approaching the natural period of heave motion, which is equal to 17.1 s.

ACKNOWLEDGEMENTS

This study was completed within the project ARCWIND—Adaptation and implementation of floating wind energy conversion technology for the Atlantic region, which is co-financed by the European Regional Development Fund through the Interreg Atlantic Area Programme under contract EAPA 344/2016.

REFERENCES

- Agarwal, P. & Manuel, L. 2009. Simulation of offshore wind turbine response for long-term extreme load prediction. *Engineering Structures*, 31, 2236–2246.
- Chakrabarti, S.K. 2005. *Handbook of offshore engineering*, Elsevier.
- DNV 2010 Environmental conditions and environmental loads.
- Faltinsen, O.M. 1990. *Sea Loads on Ships and Offshore Structures*, Cambridge University Press, Cambridge.
- Ferreira, J.A. & Guedes Soares, C. 2002. Modelling Bivariate Distributions of Significant Wave Height and Mean Wave Period. *Applied Ocean Research*, 24, 31–45.
- Guedes Soares, C. & Schellin, T.E. 1996. Long Term Distribution of Non-Linear Wave Induced Vertical Bending Moments on a Containership. *Marine Structures*, 6, 333–352.
- Guedes Soares, C. 1993. Long term distribution of non-linear wave induced vertical bending moments. *Marine Structure*, 6, 475–483.
- Guedes Soares, C., Garbatov, Y. & Teixeira, A.P. 2010. Methods of structural reliability applied to design and maintenance planning of ship hulls and floating platforms. In: Guedes Soares, C. (ed.) *Safety and Reliability of Industrial Products, Systems and Structures*. Taylor & Francis Group, London. pp. 191–206.
- Haver, S. 1985. Wave climate off Northern Norway. *Applied Ocean Research*, 7, 85–92.
- Huseby, A.B., Vanem, E. & Natvig, B. 2013. A new approach to environmental contours for ocean engineering applications based on direct Monte Carlo simulations. *Ocean Engineering*, 60, 124–135.
- Journée, J.M.J. & Massie, W.W. 2001. *Offshore Hydromechanics*, Delft University of Technology.
- Karimirad, M. & Moan, T. 2011. Extreme dynamic structural response analysis of catenary moored spar wind turbine in harsh environmental conditions. *Journal of Offshore Mechanics and Arctic Engineering*, 133, 041103-041103-14.
- Karmakar, D., Bagbanci, H. & Guedes Soares, C. 2016. Long-term extreme load prediction of spar and semisubmersible floating wind turbines using the environmental contour method. *Journal of Offshore Mechanics and Arctic Engineering* 138, 021601–021601-9.
- Li, Q., Gao, Z. & Moan, T. 2016. Modified environmental contour method for predicting long-term extreme responses of bottom-fixed offshore wind turbines. *Marine Structure*, 48, 15–32.
- Li, Q., Gao, Z. & Moan, T. 2017. Modified environmental contour method to determine the long-term extreme responses of a semi-submersible wind turbine. *Ocean Engineering*, 142, 563–576.
- Lucas, C. & Guedes Soares, C. 2015. Bivariate distributions of significant wave height and mean wave period of combined sea states. *Ocean Engineering*, 106, 341–353.
- Melchers, R.E. 1999. *Structural Reliability Analysis and Prediction*, Wiley.
- Moan, T., Gao, Z. & Ayala-Uraga, E. 2005. Uncertainty of wave-induced response of marine structures due to long-term variation of extratropical wave conditions. *Marine Structures*, 18, 18, 359–382.
- Nejad, A.R., Gao, Z. & Moan, T. 2013. Long-term analysis of gear loads in fixed offshore wind turbines considering ultimate operational loadings. *Energy Procedia*, 35, 187–197.
- Newman, J.N. 1977. *Marine Hydrodynamics*, Cambridge, MA: Massachusetts Institute of Technology.
- Raed, K., Karmakar, D. & Guedes Soares, C. 2016. Long-term assessment of the wave load acting on semi-submersible wind turbine support structure. In: Guedes Soares, C. & Santos, T.A. (eds.) *Maritime Technology and Engineering 3*. Taylor & Francis Group, London. pp. 1125–1132.
- Robertson, A., Jonkman, J., Masciola, M., Song, H., Goupee, A., Coulling, A. & Luan, C. 2014. Definition of the semisubmersible floating system for phase II of OC4 National Renewable Energy Laboratory (NREL), Technical Report NREL/TP-5000-60601.
- Saranyasontorn, K. & Manuel, L. 2004. Efficient models for wind turbine extreme loads using inverse reliability. *Journal of Wind Engineering and Industrial Aerodynamics*, 92, 789–804.
- Teixeira, A.P. & Guedes Soares, C. 2005. Assessment of partial safety factors for the longitudinal strength of tankers. In: Guedes Soares, C., et al. (eds.) *Maritime Transportation and Exploitation of Ocean and coastal Resources*. London: Taylor & Francis Group. pp. 1601–1609.
- Teixeira, A.P. & Guedes Soares, C. 2009. Reliability analysis of a tanker subjected to combined sea states. *Probabilistic Engineering Mechanics*, 24, 493–503.
- Vanem, E. & Bitner-Gregersen, E.M. 2015. Alternative Environmental Contours for Marine Structural Design—A Comparison Study. *Journal of Offshore Mechanics and Arctic Engineering*, 137, 051601-1-051601-8.
- Vanem, E. 2017. A comparison study on the estimation of extreme structural response from different environmental contour methods. *Marine Structures*, 56, 137–162.
- Videiro, P.M. & Moan, T. 1999. Efficient evaluation of long-term distributions. *Proceedings of the 18th International Conference on Offshore Mechanics and Arctic Engineering*. St. John's, Newfoundland, Canada. July 11–16. pp. 95–102.
- Winterstein, S.R. & Engebretsen, K. 1998. Reliability-based prediction of design loads and responses for floating ocean structures. *Proceedings of the 17th International Conference on Offshore Mechanics and Arctic Engineering*. Lisbon, Portugal. July 5–9.
- Winterstein, S.R., Ude, T.C., Cornell, C.A., Bjerager, P. & Haver, S. 1993. Environmental parameters for extreme response: Inverse FORM with omission factor. *ICOS-SAR*. Innsbruck, Austria.